High Quality Depth Refinement with Color Photometric Stereo

Songyou Peng

Supervised by:

Dr. Yvain Quéau Prof. Daniel Cremers

Computer Vision Group

Department of Computer Science

Technical University of Munich

A Thesis Submitted for the Degree of
MSc Erasmus Mundus in Vision and Robotics (VIBOT)

· 2017 ·

Abstract

The abstract will go here....

Research is what I'm doing when I don't know what I'm doing. . . .

Werner von Braun

Contents

List of Figures

List of Tables

Acknowledgments

Leave this part until I finish the whole thesis

Chapter 1

Introduction

1.1 Research Goal

1.2 Outline

Chapter 2

Background

Joint estimation of depth, reflectance and illumination for depth refinement

2.1 RGB-D Cameras

2.1.1 General

2.1.2 ASUS Xtion PRO LIVE

2.2 Shape from Shading & Photometric Stereo

2.2.1 Lambertian reflectance model

We can show the Intrinsic image decomposition as the an example of Lambertian reflectance as an informal explanation. shading is the product of the a certain kind of illumination model and the shape (surface normal) [1]

Illustrate with the an image from MIT intrinsic dataset [2]

SH model is an extension of Lambertian model

https://pdfs.semanticscholar.org/7b8d/fc5d6e276f8048bb53b4a5e0611019570f1b.pdf [3]

cite Shape From Shading Emmanuel Prados, Olivier Faugeras https://en.wikipedia.org/wiki/Lambertian_reflectance

https://www.cs.cmu.edu/afs/cs/academic/class/15462-f09/www/lec/lec8.pdf http://www.cs.virginia.edu/~gfx/Courses/2011/ComputerVision/slides/lecture20_pstereo.pdf

we assume that surfaces in a scene are Lambertian, and we parameterize the incident lighting with spherical harmonics (SH) [Wu et al. 2011] [4].

In fact, we estimate incident irradiance as a function of the surface normal, that is the incident light, filtered by the cosine with the normal. For Lambertian reflectance, the incident irradiance function is known to be smooth, and can be represented with only little error using the first nine spherical harmonics basis functions up to 2nd order [5]. (well, actually should check this one [6]) As with previous approaches, we henceforth estimate lighting from a grayscale version of I, and thus assume gray lighting with equal values in each RGB channel. In some steps, full RGB images are used, which we denote Ic. Unlike offline multi-view methods, we employ a triangulated depth map as geometry parameterization. This means there is a fixed depth pixel to mesh vertex relation, and we can express the reflected irradiance B(i, j) of a depth pixel (i, j) with normal n(i, j) and albedo k(i, j)

This sentence is from [7]

2.2.2 Surface normal

http://docs.opencv.org/2.4/modules/calib3d/doc/camera_calibration_and_3d_reconstruction.html

orthographic model perspective model

It is an ill-posed problem to estimate the normal, that's where SFS and PS are involved.

SFS: Horn

PS:

calibrated light: woodham [8] https://classes.soe.ucsc.edu/cmps290b/Fall05/readings/Woodham80c.pdf

uncalibrated light:

Hayakawa 94 [9] http://www.wisdom.weizmann.ac.il/~vision/courses/2010_2/papers/photometric_stereo.pdf start the I = albedo*light*normal 3×3 linear ambiguity

Yville 97 [10]: http://citeseerx.ist.psu.edu/viewdoc/download?doi=10.1.1.446.3648&rep=rep1&type=pdf use integrability (smoothness), reduce the ambiguity to 3-parameter ambiguity (GBR) $z(x, y) = \lambda z(x, y) + \mu x + \beta y$, which is GBR ambiguity. That's why our method works because we have initial depth z_0 and data fidelity term constrains the z to z_0, so the ambiguity equation is invalid. And in our case: PDE (Δz) -¿ integrability is implicity enforced

All the following PS method is trying to solve this ambiguity alldrin 07 [11] use entropy http://citeseerx.ist.psu.edu/viewdoc/download?doi=10.1.1.93.7264&rep=rep1&type=pdf

[12] perspective http://www.cv-foundation.org/openaccess/content_cvpr_2013/papers/Papadhimitri_A_New_Perspective_2013_CVPR_paper.pdf

[13]https://pdfs.semanticscholar.org/2cf9/088e9faa81872b355a4ea0a9fae46d3c8a08.pdf

[14] use TV http://oatao.univ-toulouse.fr/15158/1/queau_15158.pdf

2.3 Depth Map Refinement

mention Super-resolution Imaging that it is also very interesting to extend our the state-of-the-art depth refinement to real refinement.

mentioned very latest research is also related to depth refinement, using several images from different views (Yvain's and Zuozuo's Arxiv paper)

Chapter 3

Methodology

Many computer vision applications such as 3D object reconstruction or visual SLAM require the depth information from RGBD cameras. However, the results of these applications are often not unsatisfying because of the low quality of the depth acquisition from the cheap cameras. It would be gratifying if we can improve the depth quality without changing to an expensive camera. Therefore, the depth refinement techniques play an essential role here.

In this chapter, we first introduce some pre-processing techniques to fill the missing areas and reduce the noise of the input depth image. Then, we describe in detail one of the state-of-the-art depth refinement method from Or-El *et al.* [15] which we have chosen to implement as a starting point. A proposed method based on a RGB ratio model is then followed and introduced to eliminate the nonlinearity in most of modern depth enhancement method. Finally, another proposed technique which does not require any regularization terms is presented. This method has also exhibited the ability of dealing with the objects with complicated albedos and extension to depth super-resolution.

3.1 Pre-Processing

The first step for most of the image processing tasks is to pre-process the initial input image. Due to the hardware limitation of modern inexpensive RGBD sensors, there usually exist holes with missing values on the depth images. Also, the depth data is often noisy so we need to do denoising and acquire a relative smooth surface.

In this section, we will describe respectively the basic depth inpainting and denoising algorithm that we use for our pre-processing.

3.1.1 Depth inpainting

Image inpainting itself is a very mutual area and has been widely applied as a useful tool for many modern computer vision applications, e.g, restore the damaged parts of ancient paintings, or remove unwanted texts or objects in a photography [16]. Since the idea of image inpainting is to automatically replace the lost or undesired parts of an image with the neighbouring information by interpolating, we were inspired to apply it to fill in the missing depth information (Fig. 3.1).

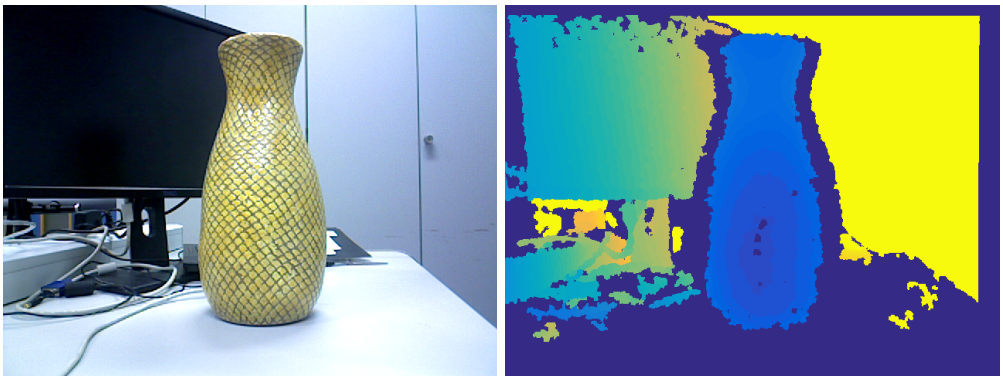

(a) RGB image (b) Input depth image

Figure 3.1: The input RGB and depth image of a vase. The brighter color on the image (b), the higher depth values.

It should be noted that, the depth inpainting is applied to the input noisy image so there is no need to use some powerful and advanced algorithms. The only request is to fill the missing areas with inexpensive computational time.

The general mathematical form of a classic inpainting algorithm [16] can be written as follows

$$I^{t+1}(i,j) = I^t(i,j) + \mu U^t(i,j), \forall (i,j) \in \Omega \tag{3.1}$$

where $I(i,j)$ is the pixel value in image I, t is the artificial time step, μ is the updating rate, U is the update information and Ω are the area with missing information.

To build the update map U in each time step, there are two principles that [16] follow. One is the inpainted values inside Ω should be as smooth as possible. The other is the lines reaching the edge of Ω should be continued and cross the missing area, while the values in Ω should be propagated from the nearest neighbours of Ω along the lines.

Again, due to the fact that our input depth images have poor quality, the lines arriving at

the boundary $\delta\Omega$ may be incorrect or produced by the noises. Thus, it is reasonable that our initial depth inpainting problem focuses on the smooth propagation from the neighbours and fill in the holes.

In each pixel (x_0, y_0) inside Ω, U can be modelled as a discrete four-neighbour Laplacian operator:

$$U(x_0, y_0) = \Delta I = 4I(x_0, y_0) - I(x_0 + 1, y_0) - I(x_0 - 1, y_0) - I(x_0, y_0 + 1) - I(x_0, y_0 - 1) \tag{3.2}$$

Now the inpainting problem in Eq. 3.1 can be represented as a minimization problem:

$$\min \iint_{\Omega} |U(x, y)|^2 dxdy \tag{3.3}$$

This problem can be reformulated to a typical linear equation in matrix form:

$$\mathbf{Ax} = \mathbf{b} \tag{3.4}$$

Assuming n is the number of pixel inside Ω and m is the sum of n and the number of neighbouring pixel around the boundary $\delta\Omega$, $\mathbf{A}$ is a $m \times n$ Laplacian matrix, $\mathbf{b}$ is a $m \times 1$ vector containing all the known boundary depth values and the 0 inside Ω. Solving the linear equation with simple least square method, we can acquire the inpainted values. With our this naive image inpainting algorithm, we can fill the holes on the depth image as shown in Fig. 3.2.

3.1.2 Depth denoising

the depth images acquired from the RGB-D cameras with moderate price usually contain various noises. As a standard pre-processing method, the image denoising technique is also applied to our input inpainted depth map. Similar to the state-of-the-art depth refinement methods [15, 17–21], bilateral fitering [22] is used as our depth pre-processing smoother.

The advantages of bilateral filter is reducing the noise while preserving the edge in the input image. More than a regular Gaussian smooth filter, which uses only the difference of the image values (depth in our case) between the center pixel the neighbours, the bilateral filter also utilizes the space difference as a reference to build up the weighting function. The filtered pixel value can be modelled as a weighted sum of neighbouring pixels:

$$\hat{I}(\mathbf{x}) = \frac{1}{W} \sum_{\mathbf{y} \in \mathcal{N}} I(\mathbf{y}) e^{-\left(\frac{\|I(\mathbf{x}) - I(\mathbf{y})\|^2}{2\sigma_r^2} + \frac{\|\mathbf{x} - \mathbf{y}\|^2}{2\sigma_d^2}\right)} \tag{3.5}$$

where $\hat{I}(\mathbf{x})$ is the filtered value at pixel $\mathbf{x}$, $\mathcal{N}$ represents the neighbouring pixels with $\mathbf{x}$ in the center, and W is the the sum of the all the weights. The smoothed result on our input depth image is shown in Fig. 3.2.

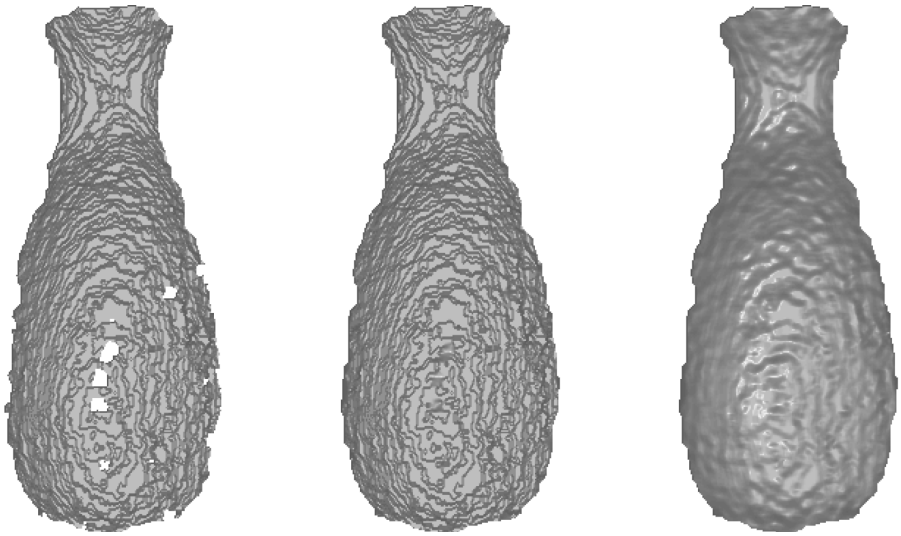

(a) Input depth (b) After inpainting (c) After smoothing

Figure 3.2: Illustrations for the pre-processing on the depth of the vase.

After the pre-processing procedure, we have an initial smooth and inpainted depth image. It will be used as the input of all the depth refinement methods detailed in the following sections.

3.2 RGBD-Fusion Like method

RGBD-Fusion is a state-of-the-art depth recovery method proposed by Or-El *et al.* [15] in 2015. This novel method is adequate for natural scene illumination and able to enhance the depth map much faster than other methods. It is reasonable to gain a comprehensive understanding in the field of depth refinement by implementing this method with our own idea inside.

It is worth mentioning that we didn't just follow the paper step by step without injecting any our own ideas. For example, instead of estimating the pixel-wise ambient light with a separate energy function, we jointly calculated all four first-order spherical harmonics parameters (3 for point-source light direction and 1 for ambient light) with a simple fast least square, and the results have only negligible difference. And throughout the whole estimation process of light, albedo and depth, we only used the information within the given mask which also speeded up the algorithm. This is the reason we call our first method "RGB-Fusion Like" method

In the following part of this section, we will explain the method and more our implementation details can be found in Appendix A.

3.2.1 Light estimation

The natural uncalibrated illumination condition means the light is no longer a point light source, thus a Lambertian model is not sufficient. Basri and Jocobs [3] has found that low order spherical harmonics (SH) model can well set out the irradiance of the diffused objects under the natural scene. More specifically, the first-order SH model can capture 87.5% of natural lighting, whose form is extended from the Lambertian model:

$$I(x,y) = \rho(x,y)(\mathbf{l}^\top \mathbf{n} + \varphi) \tag{3.6}$$

where I is the irradiance of the objects, which is represented as the intensity values, ρ is the albedo, $\mathbf{l}^\top = \begin{pmatrix} l_x & l_y & l_z \end{pmatrix}$ describes the light direction and φ represents the ambient light. Here the surface normal $\mathbf{n}$ is formulated with orthographic projection, i.e.

$$\mathbf{n} = \frac{1}{\sqrt{1+|\nabla z|^2}} \begin{pmatrix} \nabla z \\ -1 \end{pmatrix} \tag{3.7}$$

∇z represents the gradient of depth image $z(x,y)$ in x and y directions. Since we have the input depth from pre-processing, initial $\mathbf{n}_0$ is known.

In the sense of intrinsic image decomposition, an image can be decomposed as the product of albedo and shading, so we can treat $\mathbf{l}^\top \mathbf{n} + \varphi$ in Eq. 3.6 as the shading $S(x,y)$. Therefore, we have:

$$S(x,y) = \mathbf{l}^\top \mathbf{n} + \varphi = \mathbf{s} \cdot \tilde{\mathbf{n}} \tag{3.8}$$

where

$$\mathbf{s} = \begin{pmatrix} \mathbf{l} \\ \varphi \end{pmatrix} \quad \tilde{\mathbf{n}} = \begin{pmatrix} \mathbf{n} \\ 1 \end{pmatrix} \tag{3.9}$$

To compute the spherical harmonics parameters, we assume the albedo ρ equals to 1 for each pixel. Since there are known intensity value and surface normal in each pixel within the mask, we will have an overdetermined least square problem:

$$\min_{\mathbf{s}} \|I - \mathbf{s} \cdot \tilde{\mathbf{n}}\|_2^2 \tag{3.10}$$

This process only need to be applied once at the beginning of the process since the least squares is not sensitive to the details on the surface, thus the estimation from the smooth surface is enough.

3.2.2 Albedo estimation

As mentioned in Chapter 2, many depth recovery methods based on SFS or photometric stereo techniques assume constant or uniform albedo. Such assumption does not fit in with the real-world objects, and hence, they perform poorly on the shape estimation for multi-albedo cases. In order to acquire a satisfying shape outcome, an effective multi-albedo estimation process is a matter of importance.

We know from Eq. 3.6 that, if we have the knowledge of input intensity and estimated shading, the albedo image can be directly obtained from I/S. However, such albedo is prone to the overfitting, which contains all the undesired spatial layout details. To resolve the overfitting problem, we should impose some restrictions on the estimation of albedo. A large amount of our daily objects have piecewise smooth appearance, which means most pieces of a layout are dominated by certain colors. Therefore, a prior that emphasizes the piecewise smoothness on the albedo should be defined.

The albedo of an object can be roughly divided to several pieces with different colors, which we treat it as the image segmentation problem to some extend. Thus, we should refer to some classic variational segmentation methods and adapt the edge preserving smoothness term to our problem. Similar to the idea in [23], an anisotropic Laplacian term is imposed to estimate the albedo. The overall regularized minimization problem for albedo estimation is:

$$\min_{\rho} \|I - \rho S\|_2^2 + \lambda_\rho \| \sum_{k \in \mathcal{N}} \omega_k (\rho - \rho_k) \|_2^2 \tag{3.11}$$

where k indicates the neighbouring index of a certain pixel, which 4-connectivity is chosen in our case. The weight ω_k is defined as below, and it is dependent to two parameters σ_I and σ_z which accounts for the discontinuity in both intensity and depth.

$$\omega_k = \exp\left(- \frac{\|I - I_k\|_2^2}{2\sigma_I^2} - \frac{\|z - z_k\|_2^2}{2\sigma_z^2} \right) \tag{3.12}$$

3.2.3 Depth enhancement

3.3 Proposed method I: RGB Ratio Model

3.3.1 Limitations

- *LEDs have to be set up far away from each other.*
- *Natural illumination is a problem.*
- *Only feasible for the simple albedo cases*

- *Non specular objects*

3.4 Proposed method II: Robust Lighting Variation Model without Regularization

3.4.1 Depth super-resolution

Chapter 4

Results and Evaluation

4.1 RGB-D Cameras

4.1.1 General

4.1.2 ASUS Xtion PRO LIVE

4.2 Shape from Shading & Photometric Stereo

4.3 Intrinsic Image Decomposition

4.4 Super-resolution Imaging

Chapter 5

Conclusion

5.1 RGB-D Cameras

5.1.1 General

5.1.2 ASUS Xtion PRO LIVE

5.2 Shape from Shading & Photometric Stereo

5.3 Intrinsic Image Decomposition

5.4 Super-resolution Imaging

Appendix A

Implementation details

1. Detail about how to build Laplacian efficiently inside the mask

Bibliography

[1] Jonathan T Barron and Jitendra Malik. Shape, illumination, and reflectance from shading. *IEEE transactions on pattern analysis and machine intelligence*, 37(8):1670–1687, 2015.

[2] Roger Grosse, Micah K Johnson, Edward H Adelson, and William T Freeman. Ground truth dataset and baseline evaluations for intrinsic image algorithms. In *Computer Vision, 2009 IEEE 12th International Conference on*, pages 2335–2342. IEEE, 2009.

[3] Ronen Basri and David W Jacobs. Lambertian reflectance and linear subspaces. *IEEE transactions on pattern analysis and machine intelligence*, 25(2):218–233, 2003.

[4] Chenglei Wu, Kiran Varanasi, Yebin Liu, Hans-Peter Seidel, and Christian Theobalt. Shading-based dynamic shape refinement from multi-view video under general illumination. In *Computer Vision (ICCV), 2011 IEEE International Conference on*, pages 1108–1115. IEEE, 2011.

[5] Ravi Ramamoorthi and Pat Hanrahan. An efficient representation for irradiance environment maps. In *Proceedings of the 28th annual conference on Computer graphics and interactive techniques*, pages 497–500. ACM, 2001.

[6] Ravi Ramamoorthi and Pat Hanrahan. On the relationship between radiance and irradiance: determining the illumination from images of a convex lambertian object. *JOSA A*, 18(10):2448–2459, 2001.

[7] Chenglei Wu, Michael Zollhöfer, Matthias Nießner, Marc Stamminger, Shahram Izadi, and Christian Theobalt. Real-time shading-based refinement for consumer depth cameras. *ACM Transactions on Graphics (TOG)*, 33(6):200, 2014.

[8] Robert J Woodham. Photometric method for determining surface orientation from multiple images. *Optical engineering*, 19(1):191139–191139, 1980.

[9] Hideki Hayakawa. Photometric stereo under a light source with arbitrary motion. *JOSA A*, 11(11):3079–3089, 1994.

[10] Alan Yuille and Daniel Snow. Shape and albedo from multiple images using integrability. In *Computer Vision and Pattern Recognition, 1997. Proceedings., 1997 IEEE Computer Society Conference on*, pages 158–164. IEEE, 1997.

[11] Neil G Alldrin, Satya P Mallick, and David J Kriegman. Resolving the generalized bas-relief ambiguity by entropy minimization. In *Computer Vision and Pattern Recognition, 2007. CVPR'07. IEEE Conference on*, pages 1–7. IEEE, 2007.

[12] Thoma Papadhimitri and Paolo Favaro. A new perspective on uncalibrated photometric stereo. In *Proceedings of the IEEE Conference on Computer Vision and Pattern Recognition*, pages 1474–1481, 2013.

[13] Thoma Papadhimitri and Paolo Favaro. A closed-form, consistent and robust solution to uncalibrated photometric stereo via local diffuse reflectance maxima. *International journal of computer vision*, 107(2):139–154, 2014.

[14] Yvain Quéau, François Lauze, and Jean-Denis Durou. Solving uncalibrated photometric stereo using total variation. *Journal of Mathematical Imaging and Vision*, 52(1):87–107, 2015.

[15] Roy Or-El, Guy Rosman, Aaron Wetzler, Ron Kimmel, and Alfred M Bruckstein. Rgbd-fusion: Real-time high precision depth recovery. In *Proceedings of the IEEE Conference on Computer Vision and Pattern Recognition*, pages 5407–5416, 2015.

[16] Marcelo Bertalmio, Guillermo Sapiro, Vincent Caselles, and Coloma Ballester. Image inpainting. In *Proceedings of the 27th annual conference on Computer graphics and interactive techniques*, pages 417–424. ACM Press/Addison-Wesley Publishing Co., 2000.

[17] Qing Zhang, Mao Ye, Ruigang Yang, Yasuyuki Matsushita, Bennett Wilburn, and Huimin Yu. Edge-preserving photometric stereo via depth fusion. In *Computer Vision and Pattern Recognition (CVPR), 2012 IEEE Conference on*, pages 2472–2479. IEEE, 2012.

[18] Yudeog Han, Joon-Young Lee, and In So Kweon. High quality shape from a single rgb-d image under uncalibrated natural illumination. In *Proceedings of the IEEE International Conference on Computer Vision*, pages 1617–1624, 2013.

[19] Roy Or-El, Rom Hershkovitz, Aaron Wetzler, Guy Rosman, Alfred M Bruckstein, and Ron Kimmel. Real-time depth refinement for specular objects. In *Proceedings of the IEEE Conference on Computer Vision and Pattern Recognition*, pages 4378–4386, 2016.

[20] Mohammadul Haque, Avishek Chatterjee, Venu Madhav Govindu, et al. High quality photometric reconstruction using a depth camera. In *Proceedings of the IEEE Conference on Computer Vision and Pattern Recognition*, pages 2275–2282, 2014.

[21] Lap-Fai Yu, Sai-Kit Yeung, Yu-Wing Tai, and Stephen Lin. Shading-based shape refinement of rgb-d images. In *Proceedings of the IEEE Conference on Computer Vision and Pattern Recognition*, pages 1415–1422, 2013.

[22] Carlo Tomasi and Roberto Manduchi. Bilateral filtering for gray and color images. In *Computer Vision, 1998. Sixth International Conference on*, pages 839–846. IEEE, 1998.

[23] Wallace Casaca, Luis Gustavo Nonato, and Gabriel Taubin. Laplacian coordinates for seeded image segmentation. In *Proceedings of the IEEE Conference on Computer Vision and Pattern Recognition*, pages 384–391, 2014.